

SSTP: Efficient Sample Selection for Trajectory Prediction

Ruining Yang Yi Xu Yun Fu Lili Su
Northeastern University, Boston, MA, USA

{yang.ruini, xu.yi, l.su}@northeastern.edu yunfu@ece.neu.edu

Abstract

Trajectory prediction is a core task in autonomous driving. However, training advanced trajectory prediction models on large-scale datasets is both time-consuming and computationally expensive. In addition, the imbalanced distribution of driving scenarios often biases models toward data-rich cases, limiting performance in safety-critical, data-scarce conditions. To address these challenges, we propose the Sample Selection for Trajectory Prediction (SSTP) framework, which constructs a compact yet balanced dataset for trajectory prediction. SSTP consists of two main stages (1) **Extraction**, in which a pretrained trajectory prediction model computes gradient vectors for each sample to capture their influence on parameter updates; and (2) **Selection**, where a submodular function is applied to greedily choose a representative subset that covers diverse driving scenarios. This approach significantly reduces the dataset size and mitigates scenario imbalance, without sacrificing prediction accuracy and even improving in high-density cases. We evaluate our proposed SSTP on the Argoverse 1 and Argoverse 2 benchmarks using a wide range of recent state-of-the-art models. Our experiments demonstrate that SSTP achieves comparable performance to full-dataset training using only half the data while delivering substantial improvements in high-density traffic scenes and significantly reducing training time. Importantly, SSTP exhibits strong generalization and robustness, and the selected subset is model-agnostic, offering a broadly applicable solution. The code is available at <https://github.com/RuiningYang/SSTP>.

1. Introduction

Trajectory prediction aims to predict the future locations of agents conditioned on their past observations, which plays a key role in the domain of autonomous driving. This task is essential yet challenging due to the complex uncertain driving situations. With rapid developments in deep learning, various methods [4, 14, 16, 30, 52, 57, 61] have been proposed with promising trajectory prediction performance.

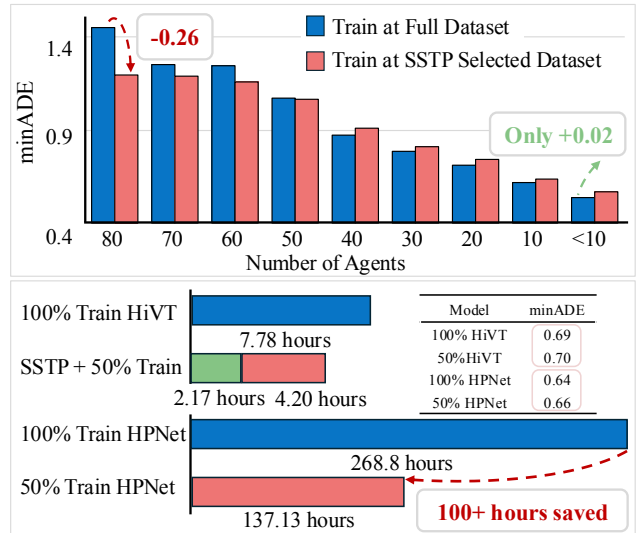


Figure 1. **Top:** Comparison of model performance across varying scene densities. Superior enhancement on HiVT-64 [61] in high-density scenarios training with SSTP-selected 50% data from Argoverse 1 [5]. **Bottom:** Using the SSTP-selected subset results in a significant overall reduction in training time compared to using the full dataset, especially for complex models like HPNet [42].

Meanwhile, more large-scale realistic datasets [1, 5, 40, 47, 49] have been released by research institute and self-driving companies, which further push the boundary of this task. However, one common issue is that training these data-driven methods requires enormous computational resources and is time-consuming due to the large scale of the datasets. For example, the recent state-of-the-art method MTR [30] has over 66 million model parameters, and the Waymo Open Motion Dataset (WOMD) [40] has over 2.2 million trajectory samples. Training the complete model on this dataset requires a substantial amount of GPU hours, posing a significant computational burden. A similar situation arises in multiple methods as well as across various datasets, which is shown in Table 1. This phenomenon raises two following questions:

Q1: Do we need large-scale datasets to train the model?

Model	Dataset	Samples	Training Time
HiVT [61]	Argoverse 1 [5]	330k	43 hours
HPNet [42]	Interaction [49]	62k	51 hours
HPNet [42]	Argoverse 1 [5]	330k	256 hours
QCNet [62]	Argoverse 2 [47]	250k	144 hours
DeMo [50]	Argoverse 2 [47]	250k	72 hours

Table 1. Statistics on the training time of trajectory prediction models and the size of the datasets used. All training time data are derived from the original experimental setup and hardware specified by the model authors.

Q2: How can we effectively reduce the training data volume without significantly compromising model accuracy?

Prompted by these questions, we take a deep dive into recent trajectory prediction benchmarks and reveal one finding: the imbalance in the dataset. From a conventional machine learning perspective, standard tasks typically evaluate model performance using the average accuracy across all samples. However, in autonomous driving trajectory prediction, this metric inherently biases models toward driving scenarios with abundant data, leading to suboptimal performance in data-scarce scenarios. For safe driving, an ideal trajectory predictor should exhibit robust performance across both data-rich and data-scarce scenarios. However, due to the imbalanced distribution of driving scenarios, existing models struggle to maintain consistent performance across diverse scenarios, as illustrated in Figure 1.

To address this issue, we introduce the Sample Selection for Trajectory Prediction (SSTP) framework, the first framework designed to construct a compact and balanced dataset for trajectory prediction. SSTP consists of two main stages: extraction and selection. In the extraction stage, a baseline model is pretrained on the full dataset for a few epochs to establish an initial feature representation. At the same time, the dataset is partitioned according to the number of agents per sample, and gradient vectors are computed for each sample to capture its influence on parameter updates. In the selection stage, we adopt a greedy strategy with a submodular function to compute scores and iteratively select representative samples. This approach builds a target subset that covers diverse driving scenarios while preserving the most distinctive features of each group. As shown in Figure 1, SSTP uniquely reduces data volume while maintaining, or even improving, model performance, particularly in high-density scenarios. Furthermore, it effectively balances the data distribution across various driving scenarios, making it well-suited for training a wide range of trajectory prediction models.

We evaluate our proposed method on the Argoverse 1 [5] and Argoverse 2 [47] datasets with multiple baseline methods. Empirical results demonstrate that SSTP successfully constructs a compact and well-balanced dataset. In

high-density scenarios, training on the selected subset significantly outperforms using the full dataset, demonstrating the effectiveness of our method. Moreover, our work offers a resource-efficient dataset that maintains balanced performance across various driving scenarios, making it well-suited for training state-of-the-art trajectory prediction models. The main contributions are summarized as follows:

- We introduce SSTP, a novel and effective framework for constructing a compact, balanced dataset for trajectory prediction, which boosts model performance across diverse driving scenarios.
- SSTP significantly reduces training time and computational cost with a one-time selection process, making it efficient and adaptable to various baseline models.
- Extensive experiments show that with only 50% of the original data, SSTP achieves comparable, or even better, performance across scenarios compared to full-dataset.

2. Related Work

2.1. Trajectory Prediction

Trajectory prediction infers an agent’s future motion from its historical observations. In recent years, research has increasingly concentrated on capturing complex multi-agent interactions, driving advances in various predictive methods [15, 23, 25, 30, 42, 43, 48, 50, 61, 62]. Furthermore, novel approaches including pretraining [7, 9, 21], historical prediction structure design [32, 42], GPT-style next-token prediction [34, 39], and post-processing optimization [10, 60] have significantly enhanced model performance, demonstrating strong results across various datasets. However, most state-of-the-art methods rely on training with large-scale datasets [1, 5, 13, 40, 47], leading to significant computational costs. In contrast, we propose a pioneering data selection strategy in the trajectory prediction domain that constructs a compact, balanced, yet highly representative dataset, significantly reducing training time while preserving model performance.

2.2. Long-Tail in Trajectory Prediction Dataset

The performance of the trajectory prediction models is evaluated based on the overall average. While they excel on benchmarks, these models often struggle with challenging scenarios [27, 35, 46] due to the long-tail data distribution, where common cases dominate and complex or rare situations are underrepresented [6]. Recent studies [22, 46, 51, 58] have started addressing the long-tail problem in trajectory prediction, primarily by leveraging contrastive learning to enhance feature representations. However, these methods mainly focus on optimizing feature-level learning while overlooking the distribution of data at the scenario level and the importance of individual samples. In contrast, our proposed method assesses the contribution of each sam-

ple and applies a refined selection strategy to build a balanced and compact dataset. Experimental results show that it significantly boosts performance in complex scenarios.

2.3. Training Sample Selection

Deep neural networks, especially Transformer-based models, depend on large-scale datasets and incur high computational costs. To reduce these costs and shorten training time, various methods focused on improving data efficiency have been proposed, including frequent parameter updates [37], fewer iterations [41], and dynamic learning rate adjustments [12, 20]. To directly reduce data volume, dataset condensation compresses raw data into compact synthetic samples [3, 19, 44, 45, 53–55]. Another widely studied approach is coreset selection, which constructs a weighted subset that closely approximates the statistical distribution of the original dataset [11, 17, 28, 29]. However, those approaches on dataset condensation [26, 31, 38, 56, 59] and coreset selection [18, 33] has been predominantly focused on image classification. In contrast, we propose a sample selection strategy based on submodular functions for the trajectory prediction domain. As a pioneering method, our approach significantly reduces the training data required while maintaining model performance.

3. Method

3.1. Problem Formulation

Consider a training set $\mathcal{D} = \{S_j\}_{j=1}^M$ consists of total M driving samples. Each sample can be described by a triple $S = (X, Y, \mathcal{O})$, where X denotes the observed trajectories, Y represents the corresponding future trajectories for all the agents present, and \mathcal{O} contains driving context information (e.g., maps). Trajectory prediction aims to estimate the future trajectory Y conditioned on X and \mathcal{O} . In this paper, our objective is to identify a smaller subset $\mathcal{C} \subseteq \mathcal{D}$ such that training a model in \mathcal{C} stays within a limited budget \mathcal{B} . We define the budget as a fraction α of the full dataset size, i.e., $\mathcal{B} = \alpha|\mathcal{D}|$. At the same time, the model trained on \mathcal{C} can achieve comparable trajectory prediction performance to that of the model trained on the full dataset \mathcal{D} .

Data Partitioning. As pointed out in Section 1, the data imbalance situation often occurs in commonly used datasets, specifically in large-scale ones. We can observe from Figure 2 that low-density scenes with few agents constitute a large portion of the dataset, while high-density scenes are underrepresented. This imbalance biases model training, making it more inclined to learn patterns from simpler scenarios while struggling to generalize to high-density scenarios. According to this observation, we first compute a density level $\rho(S_j)$ for each sample $S_j \in \mathcal{D}$ based on the number of agents present. Then, we use a fixed interval τ to partition the dataset into K disjoint subsets based on these

Algorithm 1 Sample Selection for Trajectory Prediction

Input: Full Dataset \mathcal{D} , interval τ , ratio α , submodular function $P(\cdot)$

Output: Target dataset \mathcal{C}

```

1: Initialize:  $\mathcal{C} \leftarrow \emptyset$ ;
2: Initialize:  $\mathcal{B} \leftarrow \alpha|\mathcal{D}|$ ; ▷ Set budget
3: Partitioning:  $\mathcal{D}_k$ ;
4: For  $k \in \{K, K-1, \dots, 1\}$ : ▷ Reverse order
5:    $\mathcal{C}_k \leftarrow \emptyset$ ;
6:    $n_k \leftarrow \text{DynamicBudget}(\mathcal{B}, k)$ ;
7:   if  $n_k = |\mathcal{D}_k|$  then: ▷ Include all samples
8:      $\mathcal{C} \leftarrow \mathcal{C} \cup \mathcal{D}_k$ ;
9:   else:
10:    For  $n = 1$  to  $n_k$ : ▷ Iterate  $n_k$  times
11:       $S_j \leftarrow \arg \min_{S_j \in \mathcal{D}_k \setminus \mathcal{C}_k} P(S_j)$ ;
12:       $\mathcal{C}_k \leftarrow \mathcal{C}_k \cup \{S_j\}$ ;
13:    end for
14:     $\mathcal{C} \leftarrow \mathcal{C} \cup \mathcal{C}_k$ ;
15:     $\mathcal{B} \leftarrow \mathcal{B} - |\mathcal{C}_k|$ ; ▷ Update remaining budget
16: end for
17: Return  $\mathcal{C}$ 

18: function DYNAMICBUDGET( $\mathcal{B}, k$ ):
19:   if  $|\mathcal{D}_k| \leq \lfloor \mathcal{B}/k \rfloor$  then:
20:      $n_k \leftarrow |\mathcal{D}_k|$ ;
21:   else:
22:      $n_k \leftarrow \lfloor \mathcal{B}/k \rfloor$ ;
23:   Return  $n_k$ 

```

density values. The partitioning can be defined as follows:

$$\mathcal{D} = \bigcup_{k=1}^K \mathcal{D}_k$$

$$\mathcal{D}_k = \left\{ S_j \in \mathcal{D} \mid \rho(S_j) \in [\rho_{\min} + (k-1)\tau, \rho_{\min} + k\tau) \right\}$$

$$k = 1, 2, \dots, K \quad (1)$$

where ρ_{\min} is the minimum density level in \mathcal{D} .

Gradient Extraction. We calculate the total loss as follows:

$$\mathcal{L} = \mathcal{L}_{reg} + \mathcal{L}_{cls}, \quad (2)$$

where \mathcal{L}_{reg} measures the L2 norm difference between the best mode prediction and the ground truth trajectory, and \mathcal{L}_{cls} aligns the mode predicted probabilities π with the best mode.

By backpropagating the loss \mathcal{L} , we can obtain the gradient with respect to the model output \hat{Y} as follows:

$$\nabla_{\hat{Y}} \mathcal{L} = \nabla_{\hat{Y}} (\mathcal{L}_{reg} + \mathcal{L}_{cls}). \quad (3)$$

Finally, we perform an element-wise multiplication of the calculated gradient with the corresponding decoder la-

tent vector \mathbf{E} as follows:

$$\mathbf{g} = \nabla_{\hat{\mathbf{y}}} \mathcal{L} \odot \mathbf{E}, \quad (4)$$

where \mathbf{g} captures the joint variations in the gradient and embedding spaces. In this manner, for each subset with $|\mathcal{D}_k| > n_k$, we construct a set of gradient feature vectors $\mathcal{G}_k = \{\mathbf{g}_j\}_{S_j \in \mathcal{D}_k}$ for all trajectory samples in that group.

Sample Selection. Given total K disjoint subsets and the corresponding gradient feature vectors \mathcal{G}_k , we present a submodular gain function $P(\cdot)$ to evaluate the contribution of each sample. And we utilize a greedy algorithm to iteratively construct the target dataset \mathcal{C} via optimizing the submodular gain function to ensure the selected target dataset optimally represents the entire dataset.

For each subset \mathcal{D}_k with $|\mathcal{D}_k| > n_k$, where n_k is the dynamic budget determined by the `DYNAMICBUDGET` function (see Algorithm 1), we initialize an empty set \mathcal{C}_k to store the selected samples. For these subsets, let \mathcal{G}_k denote the gradient feature vectors computed for the samples in \mathcal{D}_k . To evaluate the contribution of each sample, we define a submodular gain function based on a cosine similarity kernel. Specifically, for any trajectory sample $S_j \in \mathcal{D}_k$, the gain function is defined as follows:

$$P(S_j) = \sum_{S_i \in \mathcal{C}_k} \frac{\mathbf{g}_i \cdot \mathbf{g}_j}{\|\mathbf{g}_i\| \|\mathbf{g}_j\|} - \sum_{S_i \in \mathcal{D}_k \setminus \mathcal{C}_k} \frac{\mathbf{g}_i \cdot \mathbf{g}_j}{\|\mathbf{g}_i\| \|\mathbf{g}_j\|}, \quad (5)$$

where we use a cosine similarity kernel to measure the similarity between the sample S_j and other samples. We then apply a greedy optimization strategy, iteratively selecting the sample follows:

$$S^* = \arg \min_{S_j \in \mathcal{D}_k \setminus \mathcal{C}_k} P(S_j). \quad (6)$$

At each iteration, the selected sample S^* is added to \mathcal{C}_k . This process continues until the number of selected samples reaches the budget n_k for subset \mathcal{D}_k . Note that we process the subsets starting with those having higher density levels, as these subsets tend to contain relatively fewer samples and are underrepresented. For subsets \mathcal{D}_k where $|\mathcal{D}_k| \leq n_k$, we directly set $\mathcal{C}_k = \mathcal{D}_k$.

Finally, we can yield the target dataset $\mathcal{C} = \bigcup_{k=1}^K \mathcal{C}_k$. By incorporating gradient-based similarity into the submodular selection algorithm, our method ensures that the chosen subset maximally covers the gradient space while maintaining diversity, resulting in a smaller dataset that is both representative and informative, which ultimately leads to improved generalization in trajectory prediction models.

4. Experiments

4.1. Benchmarks and Setup

Datasets. We evaluated the effectiveness of our proposed SSTP method on Argoverse Motion Forecasting Dataset 1.1

[5] and Argoverse 2 [47]. The Argoverse 1 dataset contains 323,557 real-world driving scenarios. All the training and validation scenarios are 5-second sequences sampled at 10 Hz. The length of the historical trajectory for each scenario is 2 seconds, and the length of the predicted future trajectory is 3 seconds. The Argoverse 2 dataset contains 250,000 scenarios, with the same sampling frequency of 10 Hz. Each trajectory has a larger observation window with 5 seconds and a longer prediction horizon with 6 seconds.

Baselines. For Argoverse 1, we validate our SSTP method on two SOTA models HiVT [61] and HPNet [42] for evaluation. For Argoverse 2, we evaluate our SSTP method using two SOTA models QCNet [62] and DeMo [50]. For a more comprehensive comparison, we also include three following data selection approaches:

(1) Random Selection [36]: randomly selects a certain proportion of training samples from the original training set.

(2) K-Means Clustering [24]: clusters trajectories within the observation window based on their features, and then selects the trajectory sample closest to the cluster center in each cluster as a representative.

(3) Herding Selection [2]: a greedy strategy that first computes the mean feature of all trajectories within the observation window and then iteratively selects trajectory samples that bring the mean of the selected subset as close as possible to the overall mean.

Metrics. Following the baselines, we also generate a total 6 future trajectories and use the metrics minimum Average Displacement Error (minADE), minimum Final Displacement Error (minFDE), and Missing Rate (MR) to evaluate the prediction performance.

Implementation Details. We primarily utilized the pre-trained HiVT-64 and QCNet as backbone models to perform sample selection on the Argoverse 1 and Argoverse 2 datasets, respectively. To evaluate the performance of the selected subset, we follow their official training and validation protocols. We experimented with different selection ratios, different intervals, and assessed the prediction accuracy of the trajectory models after training on the corresponding subsets.

4.2. Main Results

Table 2 showcases the strong performance of our selected subset on the Argoverse 1 dataset across all compression rates. Following the same experimental setup as our baseline models, we trained HiVT and HPNet from scratch on the subset. When trained on the full dataset, HiVT-64 achieves a minADE of 0.695, minFDE of 1.037, and MR of 0.109. With a data retention rate of 60%, our selected subset achieves a minADE of 0.702, minFDE of 1.064, and MR of 0.110. This demonstrates that our method significantly reduces data volume while maintaining nearly lossless model performance. Even at a data retention rate of only 50%,

Methods	Ratio(%)	HiVT-64			HiVT-128			HPNet		
		minADE	minFDE	MR	minADE	minFDE	MR	minADE	minFDE	MR
Argoverse 1	100	0.695	1.037	0.109	0.666	0.978	0.091	0.647	0.871	0.070
Random	60	0.745	1.163	0.132	0.719	1.078	0.129	0.680	0.951	0.091
Cluster		0.716	1.097	0.121	0.697	1.025	0.108	0.673	0.930	0.081
Herding		0.723	1.101	0.125	0.685	1.018	0.106	0.666	0.922	0.085
SSTP (Ours)		0.702	1.064	0.110	0.674	0.994	0.093	0.653	0.901	0.071
Random	50	0.750	1.175	0.137	0.728	1.098	0.126	0.687	0.967	0.091
Cluster		0.725	1.117	0.124	0.692	1.033	0.118	0.676	0.952	0.085
Herding		0.728	1.107	0.126	0.698	1.036	0.119	0.674	0.938	0.089
SSTP (Ours)		0.704	1.073	0.111	0.684	1.022	0.101	0.661	0.913	0.074
Random	40	0.752	1.183	0.139	0.727	1.109	0.126	0.696	0.987	0.099
Cluster		0.732	1.141	0.127	0.703	1.058	0.121	0.681	0.962	0.089
Herding		0.722	1.123	0.128	0.704	1.056	0.119	0.684	0.956	0.093
SSTP (Ours)		0.711	1.088	0.114	0.696	1.048	0.106	0.671	0.931	0.076

Table 2. Performance comparison results on Argoverse 1 [5] with data retention ratios of 60%, 50%, and 40%. The compared methods include Random Selection [36], K-Means Clustering [24], and Herding Selection [2, 8]. The model used for data selection is HiVT-64 [61], while the evaluation is conducted on HiVT-64, HiVT-128, and HPNet [42]. Ratio (%) represents the proportion of retained data relative to the full training set.

Method	Ratio(%)	QCNet			DeMo		
		minADE	minFDE	MR	minADE	minFDE	MR
Argoverse 2	100	0.724	1.258	0.162	0.657	1.254	0.163
Random	60	0.787	1.419	0.208	0.755	1.433	0.198
Cluster		0.773	1.406	0.192	0.693	1.386	0.187
SSTP (Ours)		0.740	1.316	0.163	0.682	1.344	0.164
Random	50	0.805	1.447	0.219	0.756	1.448	0.203
Cluster		0.798	1.435	0.193	0.732	1.437	0.191
SSTP (Ours)		0.754	1.352	0.172	0.704	1.414	0.173
Random	40	0.811	1.471	0.226	0.763	1.475	0.202
Cluster		0.813	1.495	0.214	0.732	1.456	0.195
SSTP (Ours)		0.778	1.410	0.183	0.723	1.450	0.191

Table 3. Performance comparison results on Argoverse 2 [47] with data retention ratios of 60%, 50%, and 40%. The compared methods include Random Selection and K-means clustering. The model used for data selection is QCNet [62], while the evaluation is conducted on QCNet and DeMo [50].

models trained on our selected subset still maintain excellent performance, with minADE at 0.704, minFDE at 1.073, and MR at 0.111. Compared to random selection, our method reduces minADE by 0.046, minFDE by 0.102, and MR by 0.026. Moreover, while k-means clustering and herding methods show slight improvements in model performance, they still fall short of the performance achieved by our method. Furthermore, our subset also demonstrates superior performance on the HiVT128 model and the current SOTA model HPNet.

We further evaluated our proposed method on the Argo-

verse 2 dataset, which presents greater challenges due to its more diverse driving scenarios and longer prediction horizons. As shown in Table 3, our method consistently outperforms other data selection strategies across all data retention rates, achieving lower minADE and minFDE while maintaining a lower MR. These results further validate the robustness of our approach, as it maintains strong performance across different datasets. This demonstrates that our method is not only effective within a specific dataset but also generalizes well to more complex and diverse trajectory scenarios, such as those found in Argoverse 2.

	Agent<40			Agent>=40			Agent>=60			Agent>=80		
	minADE	minFDE	MR	minADE	minFDE	MR	minADE	minFDE	MR	minADE	minFDE	MR
Full	0.700	1.071	0.108	0.950	1.456	0.171	1.248	1.898	0.283	1.450	2.059	0.361
Random	0.734	1.127	0.119	0.997	1.552	0.193	1.287	1.989	0.315	1.638	2.359	0.389
SSTP (50%)	0.716	1.102	0.111	0.962	1.497	0.183	1.219	1.835	0.280	1.373	1.762	0.277

Table 4. Comparison of model performance across different scene densities when trained on the full dataset, random selection for 50% subset versus the 50% subset selected by our method (SSTP), where ours achieves superior performance.

Variants	Selection Strategy		Data Distribution(%)		Model Performance		
	Partition	Submodular	Agent<40	Agent>=40	minADE	minFDE	MR
Full dataset	-	-	93.88	6.12	0.692	1.047	0.104
Random	-	-	85.16	14.84	0.741	1.164	0.125
SSTP w/ Submodular		✓	93.88	6.12	0.724	1.115	0.116
SSTP w/ Partition	✓		70.35	29.65	0.729	1.116	0.118
SSTP (Ours)	✓	✓	70.35	29.65	0.704	1.073	0.111

Table 5. Performance comparison of different data selection strategies on HiVT trained with Argoverse 1. This table illustrates the impact of Partition and selection with Submodular Gain strategies on data distribution and model performance. The whole dataset and random selection serve as baselines, while different variations of SSTP are evaluated. Our method (SSTP), which integrates both strategies, achieves the best results by maintaining a balanced data distribution and reducing minADE, minFDE, and MR.

4.3. Ablation Study

Performance Enhancement. Scene density in autonomous driving varies significantly. However, most existing trajectory prediction datasets predominantly focus on low-density scenarios. From the perspective of safe driving, an ideal trajectory predictor should maintain strong performance across diverse driving scenarios, regardless of data density. To address this, we conducted a comprehensive evaluation of our proposed method on existing models and across different scene densities. As presented in Table 4, our method consistently outperforms models trained on the full dataset, particularly in high-density agent scenarios, across both Argoverse 1 and Argoverse 2 datasets. When the agent density is below 40, our method achieves comparable performance to models trained on the full dataset, with only marginal increases of 0.01 in minADE and 0.03 in minFDE, while MR remains nearly unchanged. However, in high-density scenarios where the agent count exceeds 60, models trained on our selected subset demonstrate significant improvements, with minADE and minFDE errors decreasing by over 0.03 and 0.06, respectively. This advantage becomes even more pronounced in scenarios with more than 80 agents, where minADE is reduced by approximately 0.08, minFDE by nearly 0.3, and MR by nearly 9%. Similarly, the SOTA model HPNet, when trained on our selected subset, outperforms its counterpart trained on the full dataset, demonstrating consistent improvements on the Argoverse 2 dataset.

Density Balancing. Our method explicitly controls scene

density distribution during selection, ensuring a more balanced dataset, as illustrated in Figure 2. In contrast, random selection fails to maintain this balance, resulting in an uneven distribution of scenarios with varying complexity, ultimately affecting the model’s generalization capability. As shown in Table 5 line 4, applying scene balancing alone already outperforms the random selection method. For instance, minADE decreases from 0.741 to 0.729, and minFDE drops from 1.164 to 1.116. This demonstrates that controlling scene density during data selection can enhance the effectiveness of trajectory prediction models. However, our full method outperforms scene balancing. By integrating submodular selection in addition to scene balancing, our approach further optimizes data selection by ensuring that the chosen samples carry higher information content. As a result, our method achieves minADE of 0.704 and minFDE of 1.073, further reducing errors. These findings indicate that while scene balancing is beneficial, it is insufficient to achieve optimal performance without also considering sample informativeness.

Effectiveness of Submodular Gain. To isolate the effect of submodular gain, we conducted an experiment where data selection was based solely on submodular importance scores, without considering scene density balancing, as shown in Table 5 line 3. The results indicate that using only submodular selection achieves a minADE of 0.724, lower than the 0.741 obtained through random selection, demonstrating that submodular-based sample selection improves data quality. However, it still underperforms compared to

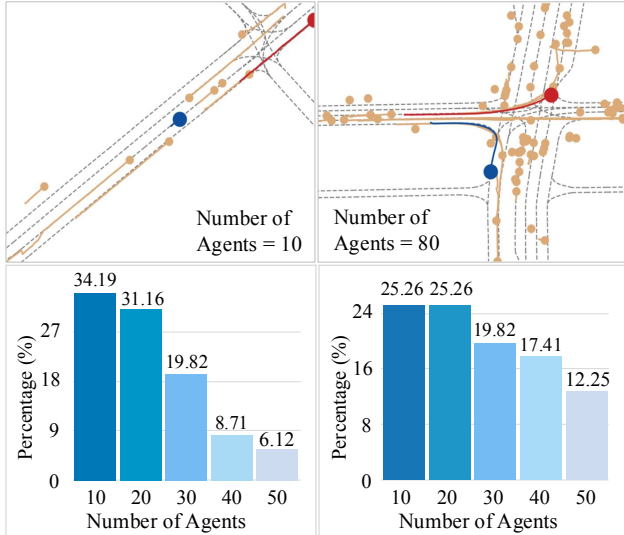


Figure 2. **Top:** Visualization examples of different driven scenarios in trajectory prediction dataset, using Argoverse 1 as an example. **Bottom:** Distribution of scene density before (**left**) and after (**right**) applying SSTP on Argoverse 1 with 50% retention ratio.

our full method. This is because prioritizing sample informativeness without adjusting for scene density leads to a dataset biased toward certain complexity levels, ultimately hindering the model’s generalization ability. In contrast, our full method, which integrates scene balancing with submodular gain, achieves the best performance across all metrics. These findings highlight the necessity of jointly considering both scene distribution balance and sample informativeness to construct an effective training dataset.

Data Retention Ratio. To examine the impact of different data retention ratios on model performance, we conducted experiments with retention rates of $\alpha = \{60, 50, 40, 30, 20, 10\}\%$ as shown in Figure 3. When higher model performance is required, retaining 50% of the data already achieves results comparable to training with on full dataset. Specifically, minADE and minFDE increase only slightly from 0.69 to 0.70, from 1.03 to 1.06, while the MR metric remains at a low level with 0.11. This demonstrates the effectiveness of our SSTP method, as the selected 50% subset is of higher quality compared to equally sized subsets selected by other methods. Furthermore, under limited computational resources, retaining only 20% of the data still yields reasonably good results. Although minADE and minFDE increase compared to the 50% subset (from 0.7063 to 0.7491 and from 1.0734 to 1.1666, respectively), the MR metric remains at 0.13. This indicates that even when the dataset size is reduced to $\frac{1}{5}$, our method can still maintain a reasonable level of predictive performance.

Impact of Pretrained Backbone Epochs. To examine the influence of the pretrained backbone on subset selection, we

Epoch	0	5	8	10	15	64
minADE	0.713	0.704	0.707	0.708	0.710	0.712
minFDE	1.083	1.073	1.076	1.074	1.083	1.080
MR	0.112	0.111	0.111	0.111	0.111	0.111

Table 6. Performance comparison of models pretrained on the full dataset for different numbers of epochs. The pretrained weights are then used to initialize the model for SSTP, selecting 50% of the data.

conducted a series of experiments using models initialized identically but trained with different numbers of pretraining epochs. Taking HiVT-64 as an example, the official training setup involves training the model for 64 epochs using the full dataset. In our experiments, we varied the number of pretraining epochs as $\{0, 5, 8, 10, 15, 64\}$ and analyzed its impact on subset selection, as shown in Table 6. The results indicate that moderate pretraining is crucial for effective subset selection. When the number of pretraining epochs is set to 5, the subset selection achieves optimal performance, consistently outperforming other configurations across all data retention ratios. As the pretraining epochs increase, subset selection continues to provide significant advantages over other data selection methods but does not surpass the performance observed at epoch 5. For models without pretraining, minADE degrades noticeably compared to models pretrained for 5 epochs. In contrast, at 64 pretraining epochs, as the model has already converged, the impact of sample selection on gradient updates diminishes. Although subset selection performance remains competitive, it does not yield further improvements over moderate pretraining.

4.4. Efficiency

Our method significantly reduces computational time while maintaining strong performance, as shown in Figure 1. On a single NVIDIA RTX 4090, training the HiVT model on the full dataset requires 7.78 hours, achieving a minADE of 0.69. In contrast, utilizing our SSTP method to select a 50% subset requires only 2.17 hours, significantly reducing the overall training time. When training on the selected subset, the total training time decreases to 6.37 hours (2.17 + 4.20), with only a minor increase of 0.01 in minADE. For the HP-Net model, full dataset training takes 307.2 hours, whereas training with the selected subset reduces the training time by over 100 hours. This decisively confirms the superior efficiency of our approach in balancing training cost and model performance.

4.5. Generalizability Study

Different Backbones. To further assess the generalizability of our method, we evaluated its performance using different backbone models. Specifically, we employed pre-trained

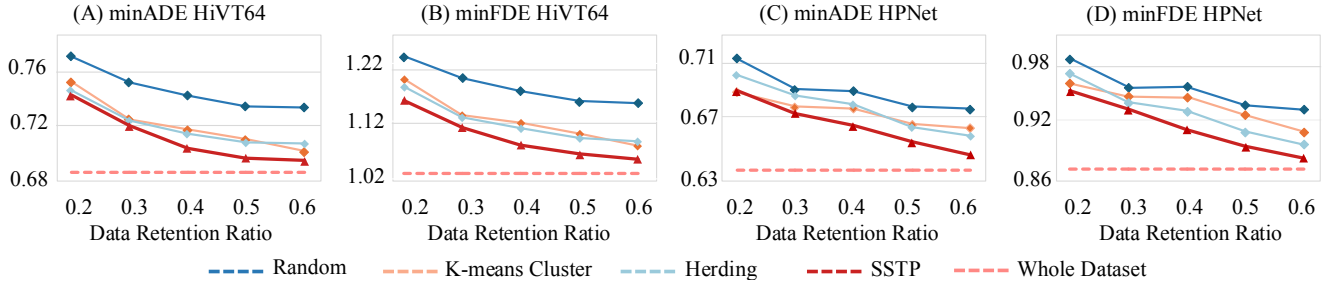


Figure 3. Performance of HiVT-64 and HPNet when training with subset chosen by different selection methods. Comparing at varying data retention ratios with minADE and minFDE. Methods include Random, K-means Clustering, Herding and SSTP, with the full dataset serving as a reference baseline. Lower values indicated better performance.

Backbone	Ratio(%)	HiVT-64			HPNet		
		minADE	minFDE	MR	minADE	minFDE	MR
HiVT-64	50	0.704	1.073	0.111	0.661	0.913	0.074
	60	0.703	1.065	0.111	0.654	0.901	0.072
HPNet	50	0.708	1.079	0.111	0.664	0.917	0.074
	60	0.703	1.067	0.108	0.657	0.910	0.075

Table 7. Performance comparison of different backbone models, HiVT-64 and HPNet, trained on selected data at varying retention rates (50% and 60%). The table reports minADE, minFDE, and MR for both models under different data selection strategies.

HiVT-64 and HPNet as feature extractors on the Argoverse 1 dataset and conducted experiments at various data retention ratios. In Table 7, we report the results for the 50% and 60% retention ratios. Additional results for other retention ratios can be found in the Supplementary Material. As shown, regardless of the backbone used for subset selection, the final trajectory prediction performance remained nearly identical. These results suggest that our subset selection strategy is largely independent of the specific feature extractor, highlighting its robustness. This broad applicability makes it a promising approach for optimizing trajectory prediction models across diverse architectures.

Partition Interval. Given the number of agents in different trajectory prediction scenarios varies significantly, we examine the impact of scene density partition intervals on the selected subset to validate the generalizability of our method. Specifically, we divide the scenes in the Argoverse 1 dataset based on agent counts with partition intervals τ of $\{5, 10, 20\}$, forming multiple scene density categories. Within each category, we perform data selection. As shown in Table 8, the subsets selected using different partition intervals result in comparable model performance, with minimal variations in minADE and minFDE. This consistency across different settings highlights the robustness of our method. This suggests that our approach generalizes well to other datasets. When applying this method, the partition interval can be adjusted based on the dataset char-

Partition	minADE	minFDE	MR
$\tau = 5$	0.703	1.056	0.110
$\tau = 10$	0.702	1.064	0.111
$\tau = 20$	0.707	1.081	0.113

Table 8. Comparison of data selected by SSTP with different partition intervals τ and its impact on HiVT performance using the Argoverse 1 dataset.

acteristics: if the dataset has relatively few agents per scene, a smaller interval is preferable; whereas for datasets with a high variance in agent count, a larger interval may be more suitable to better balance scene density.

5. Conclusion

In this paper, we presented the Sample Selection for Trajectory Prediction (SSTP) framework, a novel, data-centric approach that constructs a compact yet balanced dataset for trajectory prediction. SSTP effectively tackles the challenges posed by data imbalance and the high training costs inherent in large-scale trajectory datasets. By significantly reducing the training data volume while maintaining, and even enhancing the model performance in high-density scenarios. SSTP not only accelerates training but also delivers results comparable to, or better than, those achieved with full-dataset training. Extensive evaluations on the Argoverse 1 and Argoverse 2 benchmarks across a wide range of state-of-the-art models underscore the practical value of our approach in improving both efficiency and robustness in trajectory prediction for autonomous driving.

Limitations. Despite the effectiveness of our proposed method, improvements could be made to further reduce the computation overhead of our sample selection process. Further optimization can be made to streamline this process. Additionally, investigating methods to sustain model performance under extremely low data retention rates, e.g., 10%, presents a promising path for future research.

References

- [1] Holger Caesar, Varun Bankiti, Alex H Lang, Sourabh Vora, Venice Erin Liong, Qiang Xu, Anush Krishnan, Yu Pan, Giancarlo Baldan, and Oscar Beijbom. nuscenes: A multimodal dataset for autonomous driving. In *Proceedings of the IEEE/CVF conference on computer vision and pattern recognition*, pages 11621–11631, 2020. 1, 2
- [2] Francisco M Castro, Manuel J Marín-Jiménez, Nicolás Guil, Cordelia Schmid, and Karteek Alahari. End-to-end incremental learning. In *Proceedings of the European conference on computer vision (ECCV)*, pages 233–248, 2018. 4, 5
- [3] George Cazenavette, Tongzhou Wang, Antonio Torralba, Alexei A Efros, and Jun-Yan Zhu. Dataset distillation by matching training trajectories. In *Proceedings of the IEEE/CVF Conference on Computer Vision and Pattern Recognition*, pages 4750–4759, 2022. 3
- [4] Yuning Chai, Benjamin Sapp, Mayank Bansal, and Dragomir Anguelov. Multipath: Multiple probabilistic anchor trajectory hypotheses for behavior prediction. *arXiv preprint arXiv:1910.05449*, 2019. 1
- [5] Ming-Fang Chang, John Lambert, Patsorn Sangkloy, Jagjeet Singh, Slawomir Bak, Andrew Hartnett, De Wang, Peter Carr, Simon Lucey, Deva Ramanan, et al. Argoverse: 3d tracking and forecasting with rich maps. In *Proceedings of the IEEE/CVF conference on computer vision and pattern recognition*, pages 8748–8757, 2019. 1, 2, 4, 5
- [6] Changhe Chen, Mozghan Pourkeshavarz, and Amir Rasouli. Criteria: a new benchmarking paradigm for evaluating trajectory prediction models for autonomous driving. In *2024 IEEE International Conference on Robotics and Automation (ICRA)*, pages 8265–8271. IEEE, 2024. 2
- [7] Hao Chen, Jiase Wang, Kun Shao, Furui Liu, Jianye Hao, Chenyong Guan, Guangyong Chen, and Pheng-Ann Heng. Traj-mae: Masked autoencoders for trajectory prediction. In *Proceedings of the IEEE/CVF International Conference on Computer Vision*, pages 8351–8362, 2023. 2
- [8] Yutian Chen, Max Welling, and Alex Smola. Super-samples from kernel herding. *arXiv preprint arXiv:1203.3472*, 2012. 5
- [9] Jie Cheng, Xiaodong Mei, and Ming Liu. Forecast-mae: Self-supervised pre-training for motion forecasting with masked autoencoders. In *Proceedings of the IEEE/CVF International Conference on Computer Vision*, pages 8679–8689, 2023. 2
- [10] Sehwan Choi, Jungho Kim, Junyong Yun, and Jun Won Choi. R-pred: Two-stage motion prediction via tube-query attention-based trajectory refinement. In *Proceedings of the IEEE/CVF International Conference on Computer Vision*, pages 8525–8535, 2023. 2
- [11] Cody Coleman, Christopher Yeh, Stephen Mussmann, Baharan Mirzasoleiman, Peter Bailis, Percy Liang, Jure Leskovec, and Matei Zaharia. Selection via proxy: Efficient data selection for deep learning. *arXiv preprint arXiv:1906.11829*, 2019. 3
- [12] John Duchi, Elad Hazan, and Yoram Singer. Adaptive sub-gradient methods for online learning and stochastic optimization. *Journal of machine learning research*, 12(7), 2011. 3
- [13] Scott Ettinger, Shuyang Cheng, Benjamin Caine, Chenxi Liu, Hang Zhao, Sabeek Pradhan, Yuning Chai, Ben Sapp, Charles R Qi, Yin Zhou, et al. Large scale interactive motion forecasting for autonomous driving: The waymo open motion dataset. In *Proceedings of the IEEE/CVF International Conference on Computer Vision*, pages 9710–9719, 2021. 2
- [14] Chen Feng, Hangning Zhou, Huadong Lin, Zhigang Zhang, Ziyao Xu, Chi Zhang, Boyu Zhou, and Shaojie Shen. Macformer: Map-agent coupled transformer for real-time and robust trajectory prediction. *IEEE Robotics and Automation Letters*, 2023. 1
- [15] Francesco Giuliari, Irtiza Hasan, Marco Cristani, and Fabio Galasso. Transformer networks for trajectory forecasting. In *2020 25th international conference on pattern recognition (ICPR)*, pages 10335–10342. IEEE, 2021. 2
- [16] Junru Gu, Chen Sun, and Hang Zhao. Densetnt: End-to-end trajectory prediction from dense goal sets. In *Proceedings of the IEEE/CVF International Conference on Computer Vision*, pages 15303–15312, 2021. 1
- [17] Sarel Har-Peled and Soham Mazumdar. On coresets for k-means and k-median clustering. In *Proceedings of the thirty-sixth annual ACM symposium on Theory of computing*, pages 291–300, 2004. 3
- [18] Krishnateja Killamsetty, Sivasubramanian Durga, Ganesh Ramakrishnan, Abir De, and Rishabh Iyer. Grad-match: Gradient matching based data subset selection for efficient deep model training. In *International Conference on Machine Learning*, pages 5464–5474. PMLR, 2021. 3
- [19] Jang-Hyun Kim, Jinuk Kim, Seong Joon Oh, Sangdoon Yun, Hwanjun Song, Joonhyun Jeong, Jung-Woo Ha, and Hyun Oh Song. Dataset condensation via efficient synthetic-data parameterization. In *International Conference on Machine Learning*, pages 11102–11118. PMLR, 2022. 3
- [20] DP Kingma. Adam: a method for stochastic optimization. *arXiv preprint arXiv:1412.6980*, 2014. 3
- [21] Zhiqian Lan, Yuxuan Jiang, Yao Mu, Chen Chen, and Shengbo Eben Li. Sept: Towards efficient scene representation learning for motion prediction. *arXiv preprint arXiv:2309.15289*, 2023. 2
- [22] Zhengxing Lan, Yilong Ren, Haiyang Yu, Lingshan Liu, Zhenning Li, Yinhai Wang, and Zhiyong Cui. Hi-scl: Fighting long-tailed challenges in trajectory prediction with hierarchical wave-semantic contrastive learning. *Transportation Research Part C: Emerging Technologies*, 165:104735, 2024. 2
- [23] Junwei Liang, Lu Jiang, Kevin Murphy, Ting Yu, and Alexander Hauptmann. The garden of forking paths: Towards multi-future trajectory prediction. In *Proceedings of the IEEE/CVF conference on computer vision and pattern recognition*, pages 10508–10518, 2020. 2
- [24] Aristidis Likas, Nikos Vlassis, and Jakob J Verbeek. The global k-means clustering algorithm. *Pattern recognition*, 36(2):451–461, 2003. 4, 5
- [25] Yicheng Liu, Jinghui Zhang, Liangji Fang, Qinhong Jiang, and Bolei Zhou. Multimodal motion prediction with stacked

- transformers. In *Proceedings of the IEEE/CVF conference on computer vision and pattern recognition*, pages 7577–7586, 2021. 2
- [26] Noel Loo, Ramin Hasani, Alexander Amini, and Daniela Rus. Efficient dataset distillation using random feature approximation. *Advances in Neural Information Processing Systems*, 35:13877–13891, 2022. 3
- [27] Osama Makansi, Özgün Çiçek, Yassine Marrakchi, and Thomas Brox. On exposing the challenging long tail in future prediction of traffic actors. In *Proceedings of the IEEE/CVF International Conference on Computer Vision*, pages 13147–13157, 2021. 2
- [28] Katerina Margatina, Giorgos Vernikos, Loïc Barrault, and Nikolaos Aletras. Active learning by acquiring contrastive examples. *arXiv preprint arXiv:2109.03764*, 2021. 3
- [29] Baharan Mirzasoleiman, Jeff Bilmes, and Jure Leskovec. Coresets for data-efficient training of machine learning models. In *International Conference on Machine Learning*, pages 6950–6960. PMLR, 2020. 3
- [30] Jiquan Ngiam, Benjamin Caine, Vijay Vasudevan, Zhengdong Zhang, Hao-Tien Lewis Chiang, Jeffrey Ling, Rebecca Roelofs, Alex Bewley, Chenxi Liu, Ashish Venugopal, et al. Scene transformer: A unified architecture for predicting multiple agent trajectories. *arXiv preprint arXiv:2106.08417*, 2021. 1, 2
- [31] Timothy Nguyen, Zhoung Chen, and Jaehoon Lee. Dataset meta-learning from kernel ridge-regression. *arXiv preprint arXiv:2011.00050*, 2020. 3
- [32] Daehee Park, Jaeseok Jeong, Sung-Hoon Yoon, Jaewoo Jeong, and Kuk-Jin Yoon. T4p: Test-time training of trajectory prediction via masked autoencoder and actor-specific token memory. In *Proceedings of the IEEE/CVF Conference on Computer Vision and Pattern Recognition*, pages 15065–15076, 2024. 2
- [33] Mansheej Paul, Surya Ganguli, and Gintare Karolina Dziugaite. Deep learning on a data diet: Finding important examples early in training. *Advances in neural information processing systems*, 34:20596–20607, 2021. 3
- [34] Jonah Philion, Xue Bin Peng, and Sanja Fidler. Trajenglish: Learning the language of driving scenarios. *arXiv preprint arXiv:2312.04535*, 2(7):12, 2023. 2
- [35] Mozhgan Pourkeshavarz, Changhe Chen, and Amir Rasouli. Learn tarot with mentor: A meta-learned self-supervised approach for trajectory prediction. In *Proceedings of the IEEE/CVF International Conference on Computer Vision*, pages 8384–8393, 2023. 2
- [36] Sylvestre-Alvise Rebuffi, Alexander Kolesnikov, Georg Sperl, and Christoph H Lampert. icarl: Incremental classifier and representation learning. In *Proceedings of the IEEE conference on Computer Vision and Pattern Recognition*, pages 2001–2010, 2017. 4, 5
- [37] Herbert Robbins and Sutton Monro. A stochastic approximation method. *The annals of mathematical statistics*, pages 400–407, 1951. 3
- [38] Ahmad Sajedi, Samir Khaki, Ehsan Amjadi, Lucy Z Liu, Yuri A Lawryshyn, and Konstantinos N Plataniotis. Datadam: Efficient dataset distillation with attention matching. In *Proceedings of the IEEE/CVF International Conference on Computer Vision*, pages 17097–17107, 2023. 3
- [39] Ari Seff, Brian Cera, Dian Chen, Mason Ng, Aurick Zhou, Nigamaa Nayakanti, Khaled S Refaat, Rami Al-Rfou, and Benjamin Sapp. Motionlm: Multi-agent motion forecasting as language modeling. In *Proceedings of the IEEE/CVF International Conference on Computer Vision*, pages 8579–8590, 2023. 2
- [40] Pei Sun, Henrik Kretzschmar, Xerxes Dotiwalla, Aurelien Chouard, Vijaysai Patnaik, Paul Tsui, James Guo, Yin Zhou, Yuning Chai, Benjamin Caine, et al. Scalability in perception for autonomous driving: Waymo open dataset. In *Proceedings of the IEEE/CVF conference on computer vision and pattern recognition*, pages 2446–2454, 2020. 1, 2
- [41] Ilya Sutskever, James Martens, George Dahl, and Geoffrey Hinton. On the importance of initialization and momentum in deep learning. In *International conference on machine learning*, pages 1139–1147. PMLR, 2013. 3
- [42] Xiaolong Tang, Meina Kan, Shiguang Shan, Zhilong Ji, Jinfeng Bai, and Xilin Chen. Hpnet: Dynamic trajectory forecasting with historical prediction attention. In *Proceedings of the IEEE/CVF Conference on Computer Vision and Pattern Recognition*, pages 15261–15270, 2024. 1, 2, 4, 5
- [43] Jiangwei Wang, Lili Su, Songyang Han, Dongjin Song, and Fei Miao. Towards safe autonomy in hybrid traffic: Detecting unpredictable abnormal behaviors of human drivers via information sharing. *ACM Transactions on Cyber-Physical Systems*, 8(2):1–25, 2024. 2
- [44] Kai Wang, Bo Zhao, Xiangyu Peng, Zheng Zhu, Shuo Yang, Shuo Wang, Guan Huang, Hakan Bilen, Xinchao Wang, and Yang You. Cafe: Learning to condense dataset by aligning features. In *Proceedings of the IEEE/CVF Conference on Computer Vision and Pattern Recognition*, pages 12196–12205, 2022. 3
- [45] Tongzhou Wang, Jun-Yan Zhu, Antonio Torralba, and Alexei A Efros. Dataset distillation. *arXiv preprint arXiv:1811.10959*, 2018. 3
- [46] Yuning Wang, Pu Zhang, Lei Bai, and Jianru Xue. Fend: A future enhanced distribution-aware contrastive learning framework for long-tail trajectory prediction. In *Proceedings of the IEEE/CVF conference on computer vision and pattern recognition*, pages 1400–1409, 2023. 2
- [47] Benjamin Wilson, William Qi, Tanmay Agarwal, John Lambert, Jagjeet Singh, Siddhesh Khandelwal, Bowen Pan, Ratnesh Kumar, Andrew Hartnett, Jhony Kaesemodel Pontes, et al. Argoverse 2: Next generation datasets for self-driving perception and forecasting. *arXiv preprint arXiv:2301.00493*, 2023. 1, 2, 4, 5
- [48] Mingxing Xu, Wenrui Dai, Chunmiao Liu, Xing Gao, Weiyao Lin, Guo-Jun Qi, and Hongkai Xiong. Spatial-temporal transformer networks for traffic flow forecasting. *arXiv preprint arXiv:2001.02908*, 2020. 2
- [49] Wei Zhan, Liting Sun, Di Wang, Haojie Shi, Aubrey Claude, Maximilian Naumann, Julius Kummerle, Hendrik Königshof, Christoph Stiller, Arnaud de La Fortelle, et al. Interaction dataset: An international, adversarial and cooperative motion dataset in interactive driving scenarios with

- semantic maps. *arXiv preprint arXiv:1910.03088*, 2019. 1, 2
- [50] Bozhou Zhang, Nan Song, and Li Zhang. Decoupling motion forecasting into directional intentions and dynamic states. *Advances in Neural Information Processing Systems*, 37: 106582–106606, 2025. 2, 4, 5
- [51] Junrui Zhang, Mozghan Pourkeshavarz, and Amir Rasouli. Tract: A training dynamics aware contrastive learning framework for long-tail trajectory prediction. In *2024 IEEE Intelligent Vehicles Symposium (IV)*, pages 3282–3288. IEEE, 2024. 2
- [52] Lingyao Zhang, Po-Hsun Su, Jerrick Hoang, Galen Clark Haynes, and Micol Marchetti-Bowick. Map-adaptive goal-based trajectory prediction. In *Conference on Robot Learning*, pages 1371–1383. PMLR, 2021. 1
- [53] Bo Zhao and Hakan Bilen. Dataset condensation with differentiable siamese augmentation. In *International Conference on Machine Learning*, pages 12674–12685. PMLR, 2021. 3
- [54] Bo Zhao and Hakan Bilen. Dataset condensation with distribution matching. In *Proceedings of the IEEE/CVF Winter Conference on Applications of Computer Vision*, pages 6514–6523, 2023.
- [55] Bo Zhao, Konda Reddy Mopuri, and Hakan Bilen. Dataset condensation with gradient matching. *arXiv preprint arXiv:2006.05929*, 2020. 3
- [56] Ganlong Zhao, Guanbin Li, Yipeng Qin, and Yizhou Yu. Improved distribution matching for dataset condensation. In *Proceedings of the IEEE/CVF Conference on Computer Vision and Pattern Recognition*, pages 7856–7865, 2023. 3
- [57] Hang Zhao, Jiyang Gao, Tian Lan, Chen Sun, Ben Sapp, Balakrishnan Varadarajan, Yue Shen, Yi Shen, Yuning Chai, Cordelia Schmid, et al. Tnt: Target-driven trajectory prediction. In *Conference on Robot Learning*, pages 895–904. PMLR, 2021. 1
- [58] Weitao Zhou, Zhong Cao, Yunkang Xu, Nanshan Deng, Xiaoyu Liu, Kun Jiang, and Diange Yang. Long-tail prediction uncertainty aware trajectory planning for self-driving vehicles. In *2022 IEEE 25th International Conference on Intelligent Transportation Systems (ITSC)*, pages 1275–1282. IEEE, 2022. 2
- [59] Yongchao Zhou, Ehsan Nezhadarya, and Jimmy Ba. Dataset distillation using neural feature regression. *Advances in Neural Information Processing Systems*, 35:9813–9827, 2022. 3
- [60] Yang Zhou, Hao Shao, Letian Wang, Steven L Waslander, Hongsheng Li, and Yu Liu. Smartrefine: A scenario-adaptive refinement framework for efficient motion prediction. In *Proceedings of the IEEE/CVF Conference on Computer Vision and Pattern Recognition*, pages 15281–15290, 2024. 2
- [61] Zikang Zhou, Luyao Ye, Jianping Wang, Kui Wu, and Kejie Lu. Hivt: Hierarchical vector transformer for multi-agent motion prediction. In *Proceedings of the IEEE/CVF Conference on Computer Vision and Pattern Recognition*, pages 8823–8833, 2022. 1, 2, 4, 5
- [62] Zikang Zhou, Jianping Wang, Yung-Hui Li, and Yu-Kai Huang. Query-centric trajectory prediction. In *Proceedings of the IEEE/CVF Conference on Computer Vision and Pattern Recognition*, pages 17863–17873, 2023. 2, 4, 5